AFRL-AFOSR-UK-TR-2017-0012

Plasma Wind Tunnel Testing of Electron Transpiration Cooling Concept

Olivier Chazot
INSTITUT VON KARMAN DE DYNAMIQUE DES FLUIDES VZW

02/28/2017
Final Report

Air Force Research Laboratory
AF Office Of Scientific Research (AFOSR)/ IOE
Arlington, Virginia 22203
Air Force Materiel Command

REPORT DOCUMENTATION PAGE

Form Approved
OMB No. 0704-0188

1. REPORT DATE *(DD-MM-YYYY)*	2. REPORT TYPE	3. DATES COVERED *(From - To)*
28-02-2017	Final	01 Dec 2015 to 30 Nov 2016

4. TITLE AND SUBTITLE
Plasma Wind Tunnel Testing of Electron Transpiration Cooling Concept

5a. CONTRACT NUMBER

5b. GRANT NUMBER
FA9550-16-1-0086

5c. PROGRAM ELEMENT NUMBER
61102F

6. AUTHOR(S)
Olivier Chazot

5d. PROJECT NUMBER

5e. TASK NUMBER

5f. WORK UNIT NUMBER

7. PERFORMING ORGANIZATION NAME(S) AND ADDRESS(ES)
INSTITUT VON KARMAN DE DYNAMIQUE DES FLUIDES VZW
WATERLOOSESTEENWEG 72
SINT-GENESIUS-RODE, 1640 BE

8. PERFORMING ORGANIZATION REPORT NUMBER

9. SPONSORING/MONITORING AGENCY NAME(S) AND ADDRESS(ES)
EOARD
Unit 4515
APO AE 09421-4515

10. SPONSOR/MONITOR'S ACRONYM(S)
AFRL/AFOSR IOE

11. SPONSOR/MONITOR'S REPORT NUMBER(S)
AFRL-AFOSR-UK-TR-2017-0012

12. DISTRIBUTION/AVAILABILITY STATEMENT
A DISTRIBUTION UNLIMITED: PB Public Release

13. SUPPLEMENTARY NOTES

14. ABSTRACT
The first part of this project aimed at investigating the ETC process experimentally in the VKI Plasmatron facility on basic test materials such as graphite with a work function of approximately 4.5 eV. A provisional test design was used for testing
in the Plasmatron facility and several interesting observations could be made during this first initial test campaign. The next steps towards an improved setup would be a better electrical insulation at higher temperatures (such as alumina, up to 1500 C)
and a graphite collector to avoid pollution of the copper coil during each test run. Such a setup would require an electride material with lower work function instead of graphite as it is planned for future testing.

15. SUBJECT TERMS
EOARD, Gas-Surface Interaction, high temperature materials

16. SECURITY CLASSIFICATION OF:			17. LIMITATION OF ABSTRACT	18. NUMBER OF PAGES	19a. NAME OF RESPONSIBLE PERSON
a. REPORT	b. ABSTRACT	c. THIS PAGE			CUMMINGS, RUSSELL
Unclassified	Unclassified	Unclassified	SAR	19	19b. TELEPHONE NUMBER *(Include area code)* 011-44-1895-616021

Standard Form 298 (Rev. 8/98)
Prescribed by ANSI Std. Z39.18

von Karman Institute for Fluid Dynamics
Aeronautics and Aerospace Department

Chauseé de Waterloo, 72
B-1640 Rhode Saint Genèse
Belgium

Internal Ref: ARR 1605

February 2017

Plasma Wind Tunnel Testing of Electron Transpiration Cooling Concept

Final Performance Report

Authors: B. Helber, O. Chazot

von Karman Institute for Fluid Dynamics

Award number: FA9550-16-1-0086

Abstract

An alternative approach considered for thermal management on hypersonic planes makes use of the thermionic electron emission phenomenon, which induces a flow of electrons from the surface once the thermal energy overcomes the binding potential (work function) of the material. Efficient cooling by this Electron Transpiration Cooling (ETC) process requires electrically conductive surfaces and the ability to emit electrons once heated, preferably with low work function. This report summarizes the recent developments on ETC testing undertaken at the VKI in the inductively coupled Plasmatron facility.

The first part of this project aimed at investigating the ETC process experimentally in the VKI Plasmatron facility on basic test materials such as graphite with a work function of approximately 4.5 eV. A provisional test design was used for testing in the Plasmatron facility and several interesting observations could be made during this first initial test campaign. The next steps towards an improved setup would be a better electrical insulation at higher temperatures (such as alumina, up to 1500 C) and a graphite collector to avoid pollution of the copper coil during each test run. Such a setup would require an electride material with lower work function instead of graphite as it is planned for future testing.

Contents

Acronyms

CSU	Colorado State University
ETC	Electron Transpiration Cooling
LHTS	Local Heat Transfer Simulation
LTE	Local Thermodynamic Equilibrium
RCC	Reinforced Carbon-Carbon
TPS	Thermal Protection System
TPM	Thermal Protection Material

1. Introduction

Future hypersonic planes will require sharp leading edges with high lift-to-drag ratio in order to maximize flight range, which is achieved with a small edge radius. However, the high, localized heating caused by the aerothermal heat flux on such sharp leading edges requires enduring materials that are able to withstand the strong heating. This dependence was demonstrated by Fay and Riddell, who showed that stagnation point heat transfer is inversely proportional to the square root of the radius of the vehicle leading edge [1]. For spacecraft entering a planet's atmosphere, a Thermal Protection System (TPS) shields the substructure from the intense heating. Current Thermal Protection Material (TPM) may be reusable and can survive multiple atmospheric entries or ablative. Examples for reusable TPM are the LI-900 ceramic tiles ($T_{\max}$ =1530 K) made of silica fibers (Space Shuttle under surface) as well as a Reinforced Carbon-Carbon (RCC) composite ($T_{\max}$ =1800 K) for the wing and nose leading edges [2]. However, those materials are only used in blunt configurations and are inappropriate for the sharp leading edges on hypersonic planes.

An alternative approach that is now considered for thermal management on hypersonic planes makes use of the thermionic electron emission phenomenon, which induces a flow of electrons from the surface once the thermal energy overcomes the binding potential (work function) of the material. The electrons emitted by the surface carry energy and travel through the plasma to a collector (acting as anode), where the energy is released in form of heat once the electrons enter the collector and return in a circuit to the emitter. Efficient cooling by this ETC process requires electrically conductive surfaces and the ability to emit electrons once heated, preferably with low work function. With this report, we present the recent developments in ETC experiments undertaken at the VKI in the inductively coupled Plasmatron facility.

The ETC process relies on thermionic electron emission, where the underlying process is based on electron band theory and states that electrons with high enough kinetic energy in a solid, for example, by heating, may exit the material conduction band without getting reattached. By this, they overcome the minimum amount of energy required to leave the surface, the so-called work function. A hot cathode serves as classical example, emitting electrons into a vacuum (Edison effect). The relationship between temperature and emitted current density is formulated in Richardson's law,

$$J_{\mathrm{e}} = A_{\mathrm{R}} T_{\mathrm{w}}^2 \exp\left(\frac{-\Phi}{\mathrm{k_B T_w}}\right) \tag{1}$$

where J_{e} is the emission current density, T_{w} is the wall temperature, Φ is the work function, k_{B} is the Boltzmann constant (in eV), and A is a material dependent constant mostly assumed to be equal to $1.2 \times 10^6\,\mathrm{A/(m^2 \cdot K^2)}$. As the work function is directly linked to the atomic configuration at the surface it varies based on the material. A low work function on the order of 2.0-2.5 eV in combination with tolerance for high temperatures and oxidizing atmospheres are main requirements for the materials under consideration for ETC. Currently, new ceramic electride materials are being developed as electron emitters [3] with low enough work function for sufficient thermionic emission. During the earlier days of space flight, researchers already investigated thermionic emission on reentry vehicles with the purpose to develop a hypersonic plasma power generator [4]. But the physical phenomena associated with the proposed composite material open new opportunities for an efficient cooling of critical parts on high-speed vehicles. Several recent theoretical [5] and numerical studies [6, 7, 8] have shown the possibility of strong cooling effects through electron transpiration for the application on hypersonic vehicles.

However, all experimental data still originates from the experiments carried out in the late 60s by Touryan [9, 4]. Therefore, the first part of this project aims at investigating the ETC process experimentally in the VKI Plasmatron facility on basic test materials such as graphite with a work function of approximately 4.5 eV. The future prospects will be experimental testing of a model made of electride composite material with low working function, with the target to

record evidence of electron transpiration cooling phenomena in a flight relevant environment. Such database is expected to provide test cases for the assessment of the numerical tools developed to study the thermo-ionic emission phenomena on TPS surface temperature. This project is proposed to be conducted in collaboration with Lockheed Martin which is involved in the development of the composite material to be tested.

This report includes four main parts:

1. Definition and characterization of ground testing conditions (based on literature) (Sec. 2),
2. design of sample model (based on Touryan's experiments) and adaptation of probe holder (Sec. 3),
3. ceramic electric material testing in plasma environment (not performed),
4. measurements and analysis of the Electron Transpiration Cooling (Sec. 4.2).

2. Ground testing definition and characterization (WP 1)

First we will review probable flight conditions for application of the ETC phenomenon, used by other researchers in the literature, to be reproduced on ground in the Plasmatron test facility. Ideally, this test condition will be used with a electride material appropriate for ETC testing.

The subsequent section presents the actual test condition produced by the Plasmatron facility for testing a graphite sample.

2.1. Real flight similitude

The closest application of this technique would be hypersonic planes, scramjets, etc., that means for a generic flight object:

1. sharp leading edges (high BL gradient due to low radius)
2. 'moderate' velocities (enthalpy approx. 10 - 20 MJ/kg^3)
3. altitude only below 100 km

For example, the condition presented in Table 1 is taken from Alkandry & Boyd [6]:

Table 1: Generic freestream condition of a hypersonic plane for ETC application [6].

velocity [m/s]	altitude [km]	enthalpy [MJ/kg^3]	total pressure [hPa]
6000	67.5	18.0	38.2

To estimate the required test conditions, we made use of the Local Heat Transfer Simulation (LHTS) methodology, presented in Appendix A, which allows for a complete reproduction of the stagnation point boundary layer properties in the ground facility [10].

Plasma flow field simulations following this procedure have carried out before the experiment to pre-estimate the required ground test condition. The following procedure has been applied:

1. Flight conditions from reference and scaled to ground based on Mach number and velocity at certain altitude, providing total pressure and enthalpy.
2. This condition is close to a Plasmatron condition at 1 MW/m^2 (180 kW power) at 38 mbar based on previous experience.

3. ICP simulation (resistive magnetohydrodynamics solver) of the plasma flow at this condition (180 kW at 38 mbar) provides the boundary layer edge characteristics in non-dimensional form (air and/or nitrogen) (Appendix A).

4. those can be used with the VKI 1D boundary layer code for computation of enthalpy and boundary layer parameters:
   a) iterate on 'virtually measured' heat flux,
   b) once enthalpy is close enough to 18 MJ/kg^3 we iterate on p_{dyn} to find possible test condition,
   c) the fixed power of the ICP simulation does not have much influence on NDPs.

5. **the first experiments are carried out using nitrogen to avoid strong oxidation of the graphite sample.**

The outcome of this procedure can be found in Table 2. From those results we can see that the boundary layer gradient (between 6500 and 7300 1/s) is far below the actual flight condition boundary layer gradient (∼212946 1/s for a 1 cm radius) resulting from the small nose radius in flight.

Table 2: Boundary layer code results of test condition to represent flight condition in Table 1 (ICP = 38 hPa, 90 kW torch, nitrogen, 15 mm hemisphere), with the procedure outlined above.

Heat flux [MW/m^2]	p_{dyn} [Pa]	enthalpy [MJ/kg^3]	$\beta = du/dx$ [1/s]
1000	95	14.2	6500
1300	85	18.8	6560
1300	95	18.4	6920
1300	105	18.0	7240

2.2. Ground-test condition produced by the Plasmatron facility

The ground-test condition to be reproduced by the Plasmatron facility for a 15 mm radius hemisphere, as initially planned as test sample shape for the electride material (see below VKI design 1), was described above. This would result in a heat flux on the order of 1000-1300 kW/m^2, at a static pressure of 38 hPa with a mass flow of 16 g/s, to reproduce flight conditions presented in Table 1.

However, due to a long procurement time for the electride material, as well as for adequate alumina insulation, a graphite sample with larger radius of 25 mm was used for the this test phase. This meant that the surface temperature, and therefore, heat flux, had to be further increased in order to see any thermionic emission for the test sample (further discussed below in Fig. 2). It was further decided to use nitrogen gas instead of air, which would not have a too significant impact on the gas chemistry (degrees of dissociation and ionization), but would substantially help to prevent oxidation of the graphite surface at those elevated temperatures.

Most experiments have been carried out at heat flux levels on the order of 3 MW/m^2. The test condition, including Plasmatron generator power, static pressure, mass flow, and plasma flow rebuilding is summarized below in Table 3.

Table 3: **Plasmatron experimental test conditions**: static pressure p_s, dynamic pressure p_d, generator power P_{el}; and **numerical boundary layer edge characterization**: enthalpy h_e, density ρ_e, temperature T_e, velocity v_e, boundary layer thickness δ_e, velocity gradient β_e, Dominating mole fractions x_i.

p_s	p_d	P_{el}	h_e	ρ_e	T_e	v_e	δ_e	β_e	$[N_2]$	$[N]$	$[N^+]$	$[e^-]$
hPa	Pa	kW	MJ/kg	g/m^3	K	m/s	mm	1/s	-	-	-	-
15	260	350	60	0.25	9200	590	5.2	38150	0	0.833	0.084	0.084

3. Test assembly design (WP 2)

We will below review the best configuration proposed by Touryan's concept and previous works. This is followed by the two designs planned for testing in the Plasmatron facility. For simplicity, only VKI design 2 was used for the experiments.

3.1. Touryan best configuration

The following parameters are taken from Touryan's experiments, promising best output results.

3.1.1. Emitter area

For Touryan: $A = 5 - 20\,\mathrm{cm}^2$

VKI (1): $A = 4\pi R^2/2 = 14\,\mathrm{cm}^2$, with $R = 15\,\mathrm{mm}$ (small hemisphere)
VKI (2): $A = 4\pi R^2/2 = 39\,\mathrm{cm}^2$, with $R = 25\,\mathrm{mm}$ (big hemisphere)

3.1.2. Emitter to collector area ratio

Touryan best results $\beta = 0.1$, no effect $< 0.1 \rightarrow$ suggested to only use 'wetted' area (by visual observation)

VKI (first design, see Fig. 1):
$A_{\mathrm{cylinder}} = 132\,\mathrm{cm}^2$
$A_{\mathrm{cone}} = (R + r)\pi \cdot l, l = ((R - r)2 + h^2)) \cdot 0.5 = 106.3\,\mathrm{cm}^2 (\mathrm{l} = 4.23\,\mathrm{cm}^2)$
$A_{\mathrm{total}} = 238.3\,\mathrm{cm}^2 \rightarrow \beta = 0.05$

VKI (second design, see Fig. 3):
$A_{\mathrm{coil,wetted}} = 2\pi R \cdot l = 132\,\mathrm{cm}^2$
$\rightarrow \beta = 0.3$

3.1.3. Emitter and collector surface work function

Graphite: 4.81 eV
Copper: 4.7 eV

3.1.4. Emitter and collector surface temperature

optimum output: ratio less than 0.8 (otherwise too high back emission)
$T_e = 2100 \rightarrow T_c < 1680$
$T_e = 2300 \rightarrow T_c < 1840$

$T_e = 2500 \rightarrow T_c < 2000$
cone angle < 20 deg (VKI 30 deg)

3.1.5. Ideal results (Touryan)

Blunted cone
6-10 deg conical afterbody
$\beta \leq 0.15$
Graphite or Tungsten surface

3.2. VKI design

Two different test designs are shown below. Only VKI design 2 was used for the experiments.

3.2.1. VKI design 1

Based on the aforementioned limitations regarding emitter/collector sizes, and expected temperatures, the initial design was based on graphite emitter and collector following small hemispherical test samples of 15 mm radius (Fig. 1). An alumina electrical insulator ($T_{max} = 1800$ K) should be used to insulate emitter from collector, and a Tungsten electrode is used to connect both to a variable load or volt/ammeter.

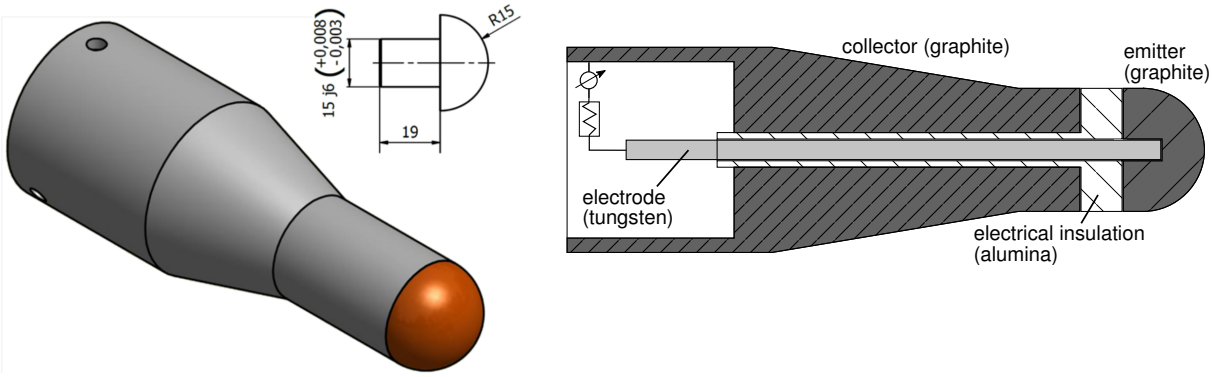

(a) (b)

Figure 1: VKI design 1: hemispherical specimen (emitter), connected by Tungsten electrode to ammeter and collector (graphite), insulator between emitter and collector could be alumina.

As procurement time of the electride composite material from Colorado State University (CSU) was unknown, graphite offered a possible backup material, based on the experiences of Touryan. Applying Eq. 1 to this geometry with a graphite work function of approximately 5 eV for increasing surface temperatures provides Fig. 2. From this we can see that in order for graphite to work as ETC emitter, surface temperatures had to be sufficiently high, i.e., higher than 2300 K to reach an emission current of 100 mA. Further, this considers the ideal case without any losses and perfect emission.

This demonstrates the high demands on the experimental design and the involved components. For example, the maximum working temperature of the above mentioned alumina electrical insulator is 1800 K and would easily be exceeded in the current design using a graphite sample.

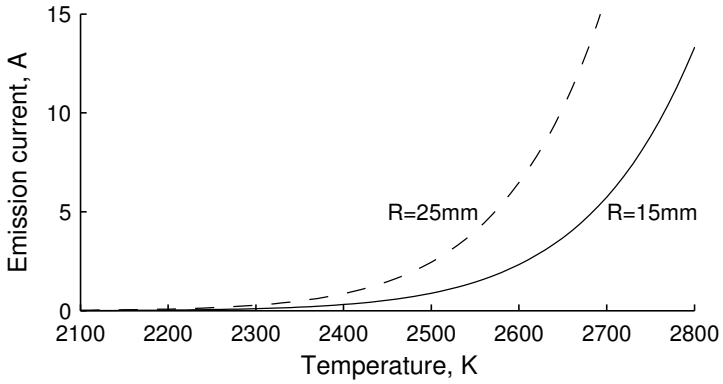

Figure 2: Theoretical thermionic emission current for VKI design 1 as a function of graphite surface temperature for two different radii: 2300 K are need to create a current of 100 mA (VKI design 1).

3.2.2. VKI design 2

Due to the long procurement time for electride material an alternative design was installed in the Plasmatron facility for the first test trial. This consisted of a 25 mm hemispherical graphite emitter, hold by a SiC-cover, which inhibits a high electric resistivity ($10^3 - 10^4\,\Omega$·m) at room temperature. However, with rising temperature the resistivity of SiC drops with a wide range of values found in literature.

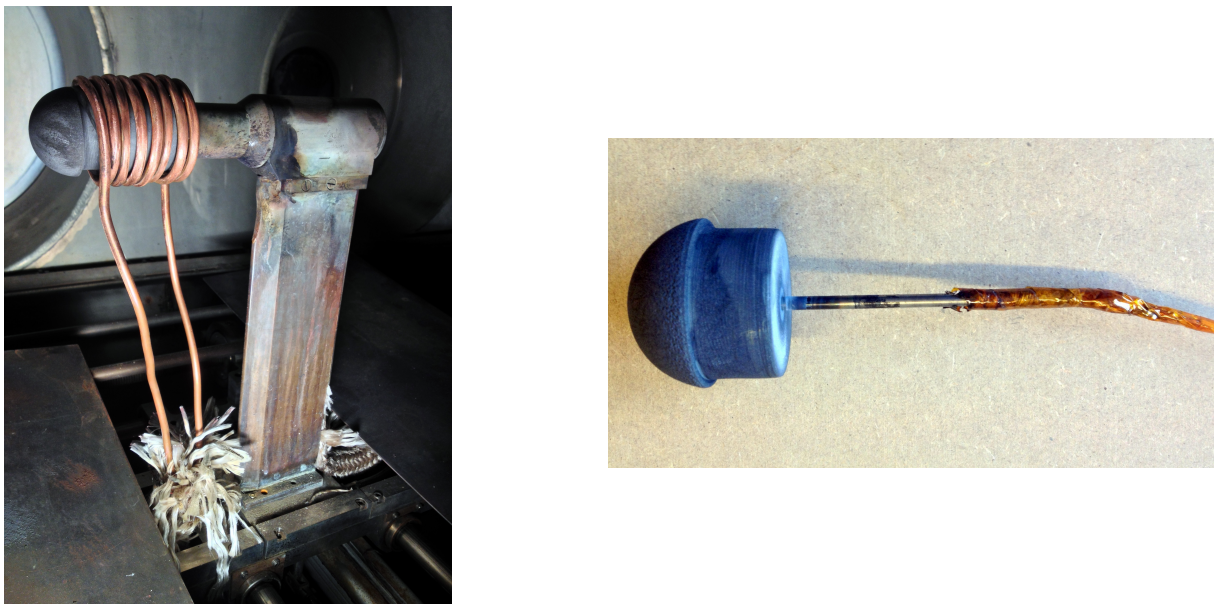

(a) (b)

Figure 3: VKI design 2: hemispherical graphite sample as emitter, SiC cover as insulator holding the sample, cooled by copper coil, acting as collector. The tungsten electrode is press-fitted into the graphite sample.

To prevent heating of the SiC holder and to act as cold collector, a water-cooled copper coil was formed around the SiC holder (Fig. 3). This coil was cleaned and polished prior to each experiment to ensure high conductivity. A tungsten rod of 100 mm length and 4 mm in diameter was used as electrode and press-fitted into the graphite emitter. The current leading wire was

wound around the electrode and electrically insulated by high-temperature resistant insulating tape in order to prevent any conduction to the holding stem. The wire was then lead outside the Plasmatron facility. Similarly, the copper coil was connected with a wire, lead outside the Plasmatron. Prior to each experiment, the electrical insulation between collector and emitter was checked.

4. Experimental description and results (WPs 3 and 4)

The last part of this report describes the actual experiments carried out, including observed features and current measurements on the graphite sample.

4.1. Plasmatron facility

The Plasmatron facility is extensively utilized at the von Karman Institute for Fluid Dynamics for the reproduction of the aero-thermodynamic environment of re-entry plasma flows, creating a high-enthalpy, highly dissociated subsonic gas flow[11]. It is equipped with a 160 mm diameter ICP (Inductively Coupled Plasma) torch powered by a high frequency, high power, high voltage (400 kHz, 1.2 MW, 2 kV) generator. In order to achieve heat fluxes higher than $\sim$5 MW/m^2, a converging nozzle can be attached to the torch of the Plasmatron (not performed for this work). As the gas is heated by induction through a coil, the advantages of ICP torches are the high purity of the plasma flows produced, due to the absence of electrodes and their associated erosion. An overview of the facility can be found in Figure 4, experimental techniques for characterization of the plasma freestream are reviewed below.

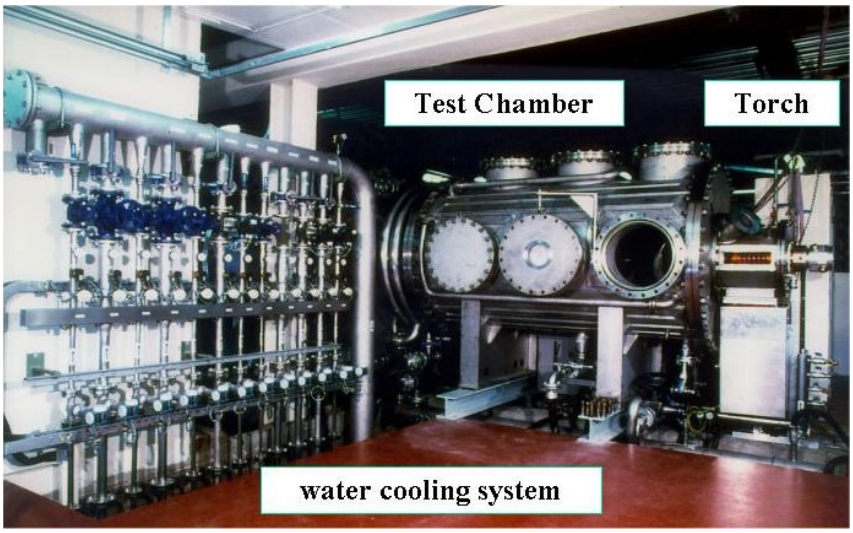

Figure 4: VKI Plasmatron test chamber overview.

A 50 mm diameter copper water-cooled probe, holding a copper calorimeter in the center of the front face, is used for the calibration of plasma flow conditions. The cold wall ($\sim$350 K) stagnation point heat flux is determined by the cooling water mass flow, controlled by a calibrated rotameter, and the inlet/outlet temperature difference, measured by two type-E thermocouples. A Teflon® insulator is inserted between the calorimeter and the probe's wall in order to have side-wall adiabatic conditions. Both the probe and calorimeter have copper surfaces which are high catalytic to nitrogen and oxygen atoms recombination. The heat flux can be measured with $\pm$10 % accuracy. A water-cooled Pitot probe is used to perform stagnation pressure mea-

surements. The pressure line is connected to a Validyne variable reluctance pressure transducer and a voltage demodulator amplifies the output. Beside the calorimeter and dynamic pressure probe for free-stream characterization, the experimental setup included surface temperature measurements using a two-color pyrometer. Validyne and amplifier are calibrated prior to the test by means of a Betz water manometer, leading to an uncertainty of ±0.2 %. The Plasmatron chamber is also equipped with an absolute pressure transducer that measures the static pressure with ±2 Pa accuracy. The probes are mounted inside the Plasmatron test chamber at 0.445 m distance from the ICP torch exit. The placement ensures that the axis of the probe and the axis of the torch itself coincide.

The mass flow was kept at $\dot{m} = 16$ g/s of nitrogen. Plasmatron test conditions providing test gas, static and dynamic pressure, cold wall heat flux, test time and surface temperature will be listed in the final paper version. The sample was attached to a sample holder located 445 mm downstream of the plasma jet exit.

4.2. Preliminary results

We performed several test runs in pure nitrogen plasma with the configuration presented above (VKI design 2, Sec. 3.2.2), heating the graphite sample up to between 2300 K to 2500 K. Examples of constant surface temperature measurements preformed by two-color pyrometry are given in Fig. 5 (a). The two-color pyrometer was focused on the samples stagnation point area with a spot size of approximately 14 mm in diameter. A graphite work function in the order of 5 eV, would, according to Eq. 1, at least theoretically be able to produce thermionic emission currents in the order of 1 A (Fig. 2).

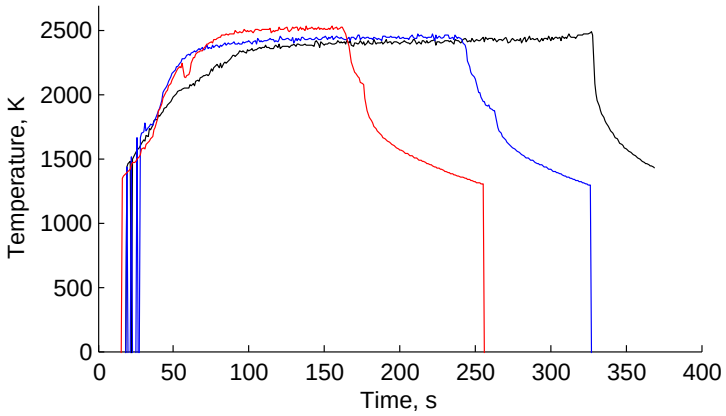

Figure 5: Surface temperature histories of several test runs in Plasmatron using graphite (test condition and plasma flow characteristics are reviewed in Table 3.

Before each test, the non-conducting connection between emitter and collector (copper spiral) was checked using an ohmmeter (order of megaohms). In this test configuration, the collector was in contact with the grounded Plasmatron test chamber, while the graphite emitter was insulated from its surroundings. The emitter was connected with the collector using an ammeter with milliampere precision in order to observe the short-circuit current. The following results have been observed:

- Once the graphite sample was injected into the plasma stream and graphite temperatures exceeded 2000 K, a small current of ∼15 mA could be measured between emitter and collector, doubling up to ∼30 mA at 2300 K surface temperature.
- We could measure a short current of 0.9 A and 1.3 A for one single experiment between collector and emitter at a surface temperature of approximately 2400 K, dropping to 10 mA

at 1900 K. However, this condition was only reached shortly at test start and could not be reproduced. The reason for this remains unsolved. One possibility is oxidation [1] / pollution of the outer surface of the cold copper collector, which had to be cleaned prior to each test run to ensure conductivity from the plasma. The slightly polluted surface after each test run was found to be not conductive anymore. Another possibility might be a change of the insulating behavior of the SiC cover, which allowed a current to flow between collector and emitter for some of the other experiments.

- In an additional test run, the ammeter was connected between the isolated graphite emitter and the ground. This yielded a short current in the order of 0.8 A, which could be reproduced during several trials. Connecting a power supply to collector and emitter, with positive pole connected to the collector, could slightly increase this current (Fig. 6). In this case the copper collector was also connected to ground, which should be avoided for improved measurements.

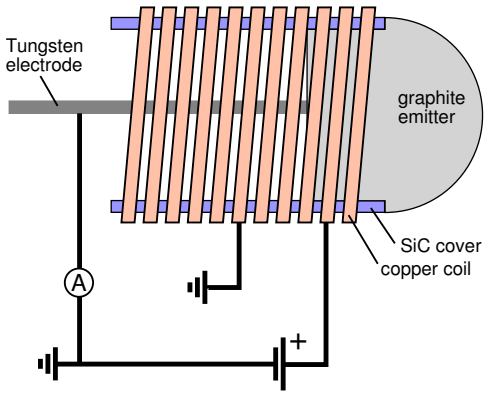

Figure 6: Schematic on ammeter and power supply connections between emitter and collector.

However, applying a potential directly between collector and emitter was not possible using the power supply because the heated plasma became conductive, creating a short circuit once the plasma was switched on. The electric conductivity of air (or nitrogen) plasma at 9200 K, which is representative of the plasma temperature for the measurements discussed above (Table 3), is approximately 2400 $1/\Omega$m (or resistivity of $\leq 0.0004\,\Omega$m), computed using our in-house library MUTATION^{++}. This is a very high conductivity compared to the contact resistances between emitter and electrodes, which were observed to be on the order of $\sim 1\,\Omega$. It was neither possible to influence the graphite surface temperature by regulating this power supply current.

The above connection (ammeter connected between ground and emitter) and consecutive measurement of a current close to one ampere suggests that the electrons emitted from the graphite may be getting collected by metal pieces somewhere downstream in the Plasmatron test chamber connected to ground, rather than reconnecting on the collector. In order to avoid such currents an entirely isolated setup would be required.

5. Concluding remarks and perspective

A provisional test design employing a 25 mm radius hemisphere graphite sample was used for ETC emission testing in the Plasmatron facility. Several interesting observations could be made during this first initial test campaign and the setup helped to understand problems associated to ETC testing:

[1] traces of oxygen remain in the test chamber due to venting from the low pressure pumps

1. Connecting and monitoring current between the emitter (graphite) and collector (copper) by an ammeter displayed a weak but increasing current with rising surface temperature.

2. For one experiment a current in the vicinity of 1 A has been observed, as predicted by Richardson's law (assuming a work function of 5 eV and a surface temperature of 2500 K).

3. A current on the order of 0.5-0.8 A was measured between the hot graphite emitter and the ground, suggesting that emitted electrodes reconnect to grounded metal parts downstream the probe rather than to the cooled copper collector.

4. The next steps towards an improved setup would be a better electrical insulation at higher temperatures (such as alumina, up to 1500 C) and a graphite collector to avoid pollution of the copper coil during each test run. However, this setup would be restricted by the low operating temperature of the alumina, which is why a more appropriate material with lower work function is expected to provide a better detection of ETC effects either by monitoring the short circuit current between emitter/collector or by varying the surface temperature through applying a potential on the specimen.

5. The strong electromagnetic field of the Plasmatron torch and associated leakage currents make sensitive measurements (order of tens of mA) in the test chamber difficult. Especially for experiments at high heat flux as reached during the graphite tests, along with low thermionic emission currents. Improved interfaces and connections of the electrodes may help to rise the weak signal measured during the experiments with graphite.

Acknowledgements

The authors are thankful to Dr. Luke A. Uribarri (Lockheed Martin), Dr. Jason Meyers (University of Vermont), Dr. Troy Holland (Colorado State University), and Kyle M. Hanquist (University of Michigan) for sharing their expertise on the topic of electron transpiration cooling and experimental design. The European Office of Aerospace Research and Development (EOARD) is acknowledged for financial support of the project under grant number FA9550-16-1-0086 (Plasma Wind Tunnel Testing of Electron Transpiration Cooling Concept for Hypersonic Vehicles). Pascal Collin is acknowledged for his valuable help as Plasmatron operator.

References

[1] Fay, J. A. and Riddell, F. R., "Theory of Stagnation Point Heat Transfer in Dissociated Air," *J. Aeronaut. Sci.*, Vol. 25, No. 2, 1958, pp. 73–85.

[2] Williams, S. D. and Curry, D. M., "Assessing the orbiter thermal environment using flight data ", Journal of Spacecraft and Rockets, Vol. 21, No. 6 (1984), pp. 534-541." *J. Spacecraft Rock.*, Vol. 21, No. 6, 1984, pp. 534–541.

[3] Yoshizumi, T. and Hayashi, K., "Thermionic Electron Emission from a Mayenite Electride-Metallic Titanium Composite Cathode," *Applied Physics Express*, Vol. 6, No. 1, December 2013.

[4] Touryan, K. J., "A Hypersonic Plasma Power Generator," *AIAA J.*, Vol. 3, No. 4, 1965, pp. 652–659.

[5] Uribarri, L. A. and Allen, E. H., "Electron Transpiration Cooling for Hot Aerospace Surfaces," *20th AIAA International Space Planes and Hypersonic Systems and Technologies Conference*, AIAA paper 2015-3674, Glasgow, Scotland, July 2015.

[6] Alkandry, H., Hanquist, K. M., and Boyd, I. D., "Conceptual Analysis of Electron Transpiration Cooling for the Leading Edges of Hypersonic Vehicles," *11th AIAA/ASME Joint Thermophysics and Heat Transfer Conference*, AIAA paper 2014-2674, Atlanta, GA, USA, June 2014.

[7] Hanquist, K. M. and Boyd, I. D., "Comparisons of Computations with Experiments for Electron Transpiration Cooling at High Enthalpies," *45th AIAA Thermophysics Conference*, AIAA paper 2015-2351, Dallas, TX, USA, June 2015.

[8] Hanquist, K. M. and Boyd, I. D., "Limits for Thermionic Emission from Leading Edges of Hypersonic Vehicles," *54th AIAA Aerospace Sciences Meeting*, AIAA paper 2016-0507, San Diego, CA, USA, January 2016.

[9] Touryan, K. J., "The Hypersonic Plasma Converter: II," Report no. sc-rr-4960, Sandia Laboratories, Albuquerque, New Mexico, USA, 1964.

[10] Kolesnikov, A. F., "Conditions of Simulation of Stagnation Point Heat Transfer from a High-enthalpy Flow," *Fluid Dyn.*, Vol. 28, No. 1, 1993, pp. 131–137.

[11] Bottin, B., Chazot, O., Carbonaro, M., van der Haegen, V., and Paris, S., "The VKI Plasmatron Characteristics and Performance," *RTO AVT Course on Measurement Techniques for High Enthalpy and Plasma Flows*, RTO EN-8, Rhode-Saint-Genèse, Belgium, October 1999, pp. 6–01 – 6–26.

[12] Barbante, P. and Chazot, O., "Flight Extrapolation of Plasma Wind Tunnel Stagnation Region Flowfield," *J Thermophys Heat Transfer*, Vol. 20, No. 3, 2006, pp. 493–499.

[13] Degrez, G., Barbante, P., de la Llave, M., Magin, T. E., and Chazot, O., "Determination of the catalytic properties of TPS Materials in the VKI ICP Facilities," *ECCOMAS Computational Fluid Dynamics Conference*, Swansea, Wales, UK, September 2001.

[14] Goulard, R., "On Catalytic Recombination Rates in Hypersonic Stagnation Heat Transfer," *Jet Propul.*, Vol. 28, 1958, pp. 737–745.

[15] Anderson, J. D. J., *Hypersonic and High Temperature Gas Dynamics*, McGraw-Hill, New York, 1989.

[16] Degrez, G., Vanden Abeele, D. P., Barbante, P. F., and Bottin, B., "Numerical Simulation of Inductively Coupled Plasma Flows under Chemical Non-equilibrium," *Int. J. Numer. Meth. Heat. Fluid Flow*, Vol. 14, No. 4, 2004, pp. 538–558.

[17] Vanden Abeele, D. and Degrez, G., "Efficient computational model for inductive plasmas flows," *AIAA J.*, Vol. 38, No. 2, 2000, pp. 234–242.

[18] Magin, T., *A Model for Inductive Plasma Wind Tunnels*, Ph.D. thesis, Université libre de Bruxelles, von Karman Institute for Fluid Dynamics, 2004.

[19] Barbante, P., Degrez, G., and Sarma, G., "Computation of Nonequilibrium High Temperature Axisymmetric Boundary-Layer Flows," *J. Thermophys. Heat Transfer*, Vol. 16, No. 4, 2002, pp. 490–497.

Appendices

A. Local Heat Transfer Simulation methodology

This section serves to explain how the plasma flow produces a suitable TPM test environment.

The stagnation point region of a hypersonic reentry capsule is characterized by a subsonic, high-temperature boundary layer. A subsonic ground-test facility, such as the VKI Plasmatron, is thus able to provide a complete duplication of the reentry flight condition, as highlighted in Fig. 7. The so-called LHTS methodology was developed by Kolesnikov [10] for ICP torches at the Institute for Problems in Mechanics (IPM, Moscow, Russia) and adapted by Barbante et al. to the VKI Plasmatron [12, 13]. The concept is based on the boundary layer theory for dissociated reacting gases following the works of Fay and Riddell [1], and Goulard [14].

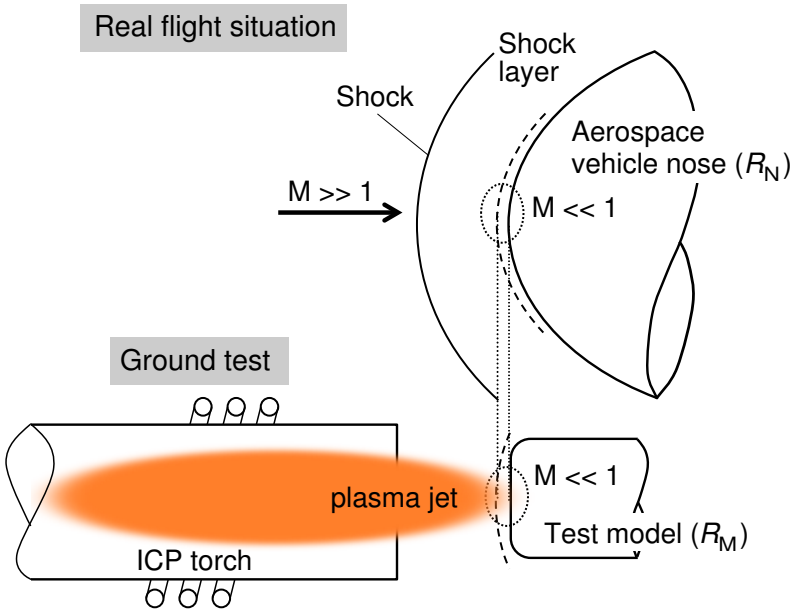

Figure 7: Use of ICP jet for TPM testing: Simplified hypersonic flow in real flight condition & subsonic plasma jet following the LHTS methodology, reproducing the stagnation point region.

Kolesnikov's works state that, under the assumption of Local Thermodynamic Equilibrium (LTE) at the outer edge of the boundary layer, the stagnation point heat flux in flight and on ground are identical, if the boundary layer edge total enthalpy H_e, the pressure p_e, and the radial velocity gradient in radial direction at the wall $\beta_e = \partial u/\partial x|_e$ are locally matched on the test sample:

$$H_e^f = H_e^t, \qquad p_e^f = p_e^t, \qquad \beta_e^f = \beta_e^t. \tag{2}$$

The superscripts f and t stand for "flight" and "test" quantities, respectively. The convention for x and u as tangential coordinate and tangential velocity to the wall origins from boundary layer theory, with y and v taken as the normal coordinate and velocity. The velocity gradient β_e is dimensionally equivalent to the inverse of a Lagrangian time of residence at the stagnation point, and allows for reproduction of the chemical conditions in flight and in the wind-tunnel. A high gradient provokes the flow to be rather frozen, while a low gradient provokes thermodynamic equilibrium.

The flight total enthalpy and pressure can be derived from the conservation of energy and

momentum on the stagnation-line,

$$h_{\mathrm{e}}^{\mathrm{f}} = h_{\infty} + \frac{1}{2}\left(v_{\infty}^{\mathrm{f}}\right)^2, \tag{3}$$

$$p_{\mathrm{e}}^{\mathrm{f}} = p_{\infty}^{\mathrm{f}} + \rho_{\infty}^{\mathrm{f}}\left(v_{\infty}^{\mathrm{f}}\right)^2, \tag{4}$$

while the velocity gradient arises from the vehicle's shape and radius,

$$\beta_{\mathrm{e}}^{\mathrm{f}} = \frac{1}{R_{\mathrm{N,eff}}}\sqrt{\frac{2\left(p_{\mathrm{e}} - p_{\infty}\right)}{\rho_{\mathrm{e}}}}. \tag{5}$$

The first terms in Eqs. 3 and 4, describing the ambient enthalpy h_{∞} and the ambient pressure p_{∞}, are negligible at hypersonic speed. An approximation of the velocity gradient β (Eq. 5) is given by the modified Newtonian Theory [15]. For non-spherical bodies (R_{N}), an effective radius $R_{\mathrm{N,eff}}$ can be used that corresponds to the radius of a sphere with equivalent velocity gradient.

A coupled numerical-experimental procedure allows for computation of the nonequilibrium boundary layer chemistry, plasma freestream enthalpy, and temperature. First, cold-wall heat flux and pitot pressure are being intrusively determined during the Plasmatron experiment at a certain generator power P_{el}. The subsonic Plasmatron flow-field is then numerically simulated using a resistive magnetohydrodynamics solver, characterizing the boundary layer geometry around the heat flux probe under LTE and axisymmetric flow assumption (VKI ICP code [16, 17, 18]). The set of magnetohydrodynamics equations combine fluid dynamics (Navier-Stokes) and electromagnetism (Maxwell) in order to compute the flow in the ICP torch and test chamber simultaneously. Input to this procedure are the gas mass flow, electrical power, and static pressure p_{s} in the test chamber. The VKI ICP code makes use of the MUTATION^{++} library to determine thermodynamic and transport properties of an eleven species air mixture, including O_2, N_2, O_2^+, N_2^+, NO, NO^+, O, O^+, N^+, N, e^-, and a five species nitrogen mixture including N_2, N_2^+, N, N^+, e^-. Figure 8 illustrates a simulated flow field for a generator power of $P_{\mathrm{el}} = 180\,\mathrm{kW}$ together with a detailed schematic of the boundary layer stagnation point region.

The boundary layer scheme highlights the velocity normal to the wall (v), the boundary layer thickness δ, and the gradient of the tangential velocity in tangential direction ($\frac{\partial u}{\partial x}$).

After simulation of the plasma flow field with the ICP code, the boundary layer edge characteristics, as well as the experimentally determined heat flux and pitot pressure, serve as input conditions for the VKI boundary layer code [19]. It solves the axisymmetric, chemically-reacting stagnation-line boundary layer over a catalytic surface under chemical nonequilibrium conditions (the computational domain can be taken as the stagnation-line in the detail of Fig. 8). A Newton method is used to iterate on the boundary layer outer edge temperature T_{e}, until experimental and numerical heat fluxes are matched,

$$\dot{q}_{\mathrm{cw}}^{(\mathrm{exp})} = \dot{q}_{\mathrm{cw}}^{(\mathrm{num})} = \dot{q}_{\mathrm{cw}}\left(\gamma_{\mathrm{ref}}, T_{\mathrm{cw}}, p_{\mathrm{e}}, T_{\mathrm{e}}, \delta, \left(\frac{\partial u}{\partial x}\right)_{\mathrm{e}}, v_{\mathrm{e}}\frac{\partial}{\partial y}\left(\frac{\partial u}{\partial x}\right)_{\mathrm{e}}\right), \tag{6}$$

with T_{cw} and γ_{ref} being the cold-wall surface temperature and the reference catalycity of the heat flux probe. The last three terms in Eq. 6 are the boundary layer edge characteristics provided by the ICP code in non-dimensional form.

Output of the whole procedure is the plasma condition at the boundary layer edge, independent of ablation at the surface.

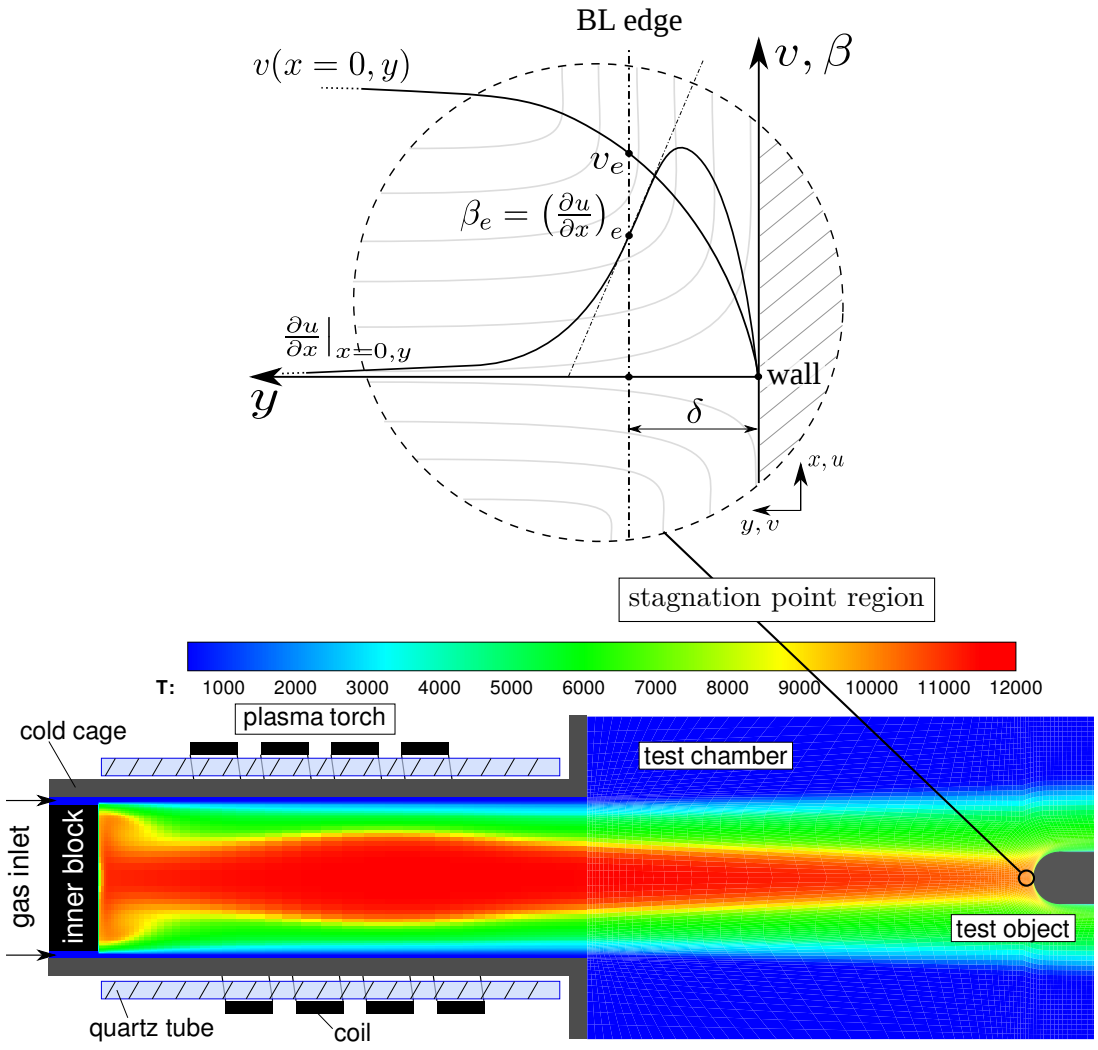

Figure 8: Axisymmetric equilibrium computation of the temperature field inside the Plasmatron torch and test chamber (air, $\dot{m} = 16\,\mathrm{g/s}$, $p_\mathrm{s} = 15\,\mathrm{hPa}$, $P_\mathrm{ICP} = 90\,\mathrm{kW}$), with detailed schematic of the stagnation point region: streamlines in light gray, normal (axial) velocity component v and tangential velocity gradient in tangential direction β_e at $x = 0$ are superimposed.